



Lung magnetic resonance imaging in systemic sclerosis: a new promising approach to evaluate pulmonary involvement and progression

Luna Gargani¹ · Cosimo Bruni² · Daniele De Marchi³ · Chiara Romei⁴ · Serena Guiducci² · Silvia Bellando-Randone² · Giovanni Donato Aquaro³ · Alessia Pepe³ · Emanuele Neri⁵ · Stefano Colagrande⁶ · Fabio Falaschi⁴ · Alberto Moggi-Pignone⁷ · Alessandro Pingitore¹ · Marco Matucci-Cerinic²

Received: 20 August 2020 / Revised: 24 October 2020 / Accepted: 29 October 2020 / Published online: 7 November 2020
© International League of Associations for Rheumatology (ILAR) 2020

Abstract

Introduction/objectives Interstitial lung disease (ILD) is frequent and highly disabling in systemic sclerosis (SSc). Magnetic resonance imaging (MRI) is not routinely used to evaluate the lung, due to poorer spatial resolution compared to high-resolution computed tomography (HRCT). We aimed to compare lung MRI signal with HRCT and evaluate the role of MRI in predicting ILD progression.

Methods Thirty SSc patients underwent lung MRI and HRCT. STIR and T1 mapping sequences were acquired before and after gadolinium injection. Patients were classified as *normal* (group 1 with normal HRCT and MRI), *discordant* (group 2 without ILD signs on HRCT but areas of hyperintensity on MRI), and *abnormal* (group 3 with ILD signs on HRCT and areas of hyperintensity on MRI). Patients were followed up for ILD progression.

Results Mean STIR and T1 values were different between the three groups ($p < 0.0001$). STIR values correlated with HRCT score ($R = 0.79$, $p < 0.0001$), lung ultrasound B-lines ($R = 0.73$, $p < 0.0001$), and %DLco ($R = -0.63$, $p = 0.0001$). Nine events were recorded during a follow-up of 25 ± 20 months. Continuous STIR values were independently associated with events (HR 1.018; CI 1.005–1.031, $p = 0.005$). A STIR value >90 ms discriminated patients at a higher risk of worsening pulmonary involvement (HR 8.80; CI 1.81–42.74; $p < 0.007$).

Conclusions Lung MRI can detect SSc-related ILD, with good correlations with other ILD markers. STIR values, independently of HRCT appearance, may predict worsening lung involvement. Lung MRI, although very preliminary, is a promising tool that in a near future could help selecting patients for an early treatment of SSc-related ILD and a more appropriate use of HRCT.

Key points

- Lung MRI has the potential to differentiate inflammation-predominant versus fibrosis-predominant lesions, but it is not currently used in routine clinical practice to assess SSc-related ILD.
- Lung MRI STIR and T1 values are significantly different between patients with and without SSc-related ILD. STIR values, independently of HRCT appearance, are also able to predict worsening lung involvement over time.
- These preliminary data suggest that, in a near future, MRI could support the choice for an early treatment of SSc-related ILD, as well as a more appropriate use of HRCT.

Luna Gargani and Cosimo Bruni contributed equally to this work.

✉ Luna Gargani
gargani@ifc.cnr.it

¹ Institute of Clinical Physiology, National Research Council, Via Moruzzi, 1, 56124 Pisa, Italy

² Department of Experimental and Clinical Medicine, Department of Geriatric Medicine, Division of Rheumatology AOUC, University of Florence, Florence, Italy

³ Department of Magnetic Resonance, Fondazione Toscana G. Monasterio, Pisa, Italy

⁴ II Radiology Unit, University Hospital of Pisa, Pisa, Italy

⁵ Diagnostic and Interventional Radiology, Department of Translational Research, University of Pisa, Pisa, Italy

⁶ Department of Experimental and Clinical Biomedical Sciences, Radiodiagnostic Unit n. 2, University of Florence - Azienda Ospedaliero-Universitaria Careggi, Florence, Italy

⁷ Department of Experimental and Clinical Medicine, Department of Emergency Medicine DEA, Division of Internal Medicine AOUC, University of Florence, Florence, Italy

Keywords Interstitial lung disease · Magnetic resonance imaging · Systemic sclerosis

Introduction

Systemic sclerosis (SSc) is a complex disease leading to fibrosis of the skin and internal organs and in particular of the lung [1, 2]. Interstitial lung disease is the leading cause of death in systemic sclerosis [3, 4]. Its diagnosis may be achieved with high-resolution computed tomography (HRCT) as a non-invasive surrogate for gold standard biopsy [5–7]. It is well known that HRCT may reflect the features of non-specific interstitial pneumonia (NSIP—characterized by a greater prevalence ground-glass opacities (GGO) than coarse reticulation (RET)) or, less frequently, of usual interstitial pneumonia pattern (UIP—with sub-pleural basal predominance of RET and honeycombing (HC), with or without traction bronchiectasis) [8, 9]. In order to reduce radiation exposure, magnetic resonance imaging (MRI) was proposed as a radiation-free technique to detect morphological and functional findings of parenchymal lung disease [10]. Lung MRI has the potential to differentiate inflammation-predominant versus fibrosis-predominant lesions, and during the past decade, significant developments have been achieved in this field with promising preliminary data on its potential employment in the assessment of many pulmonary diseases. Lung MRI has been indeed performed in patients with ILD of different aetiologies, from connective tissue disease (CTD)—related ILD (including SSc) to idiopathic pulmonary fibrosis (IPF) and sarcoidosis [11, 12]. In these contexts, lung MRI was shown to be comparable or inferior to HRCT in the morphological evaluation of typical ILD changes (including ground-glass opacities (GGO), reticulation (RET), and honeycombing (HC)) [11]. Promising data are available for lung MRI to distinguish between lung segments with active and non-active inflammation; despite limited evidences being available for detection of inflammation in IPF and sarcoidosis, lung MRI has proven to be useful in the assessment of lung ventilation changes, as well as in the assessment of lymph nodes' involvement [12]. Conversely, short tau inversion recovery (*STIR*) sequences can detect oedema with high specificity, and T1 mapping assessment can detect tissue abnormalities with high sensitivity, especially in CTD-related ILD [11].

However, at present, MRI use is limited compared to HRCT, in particular for technical issues due to vascular, respiratory, and body movements as well as a lower spatial resolution [13]; thus, it is not routinely employed for the evaluation of the lung, although it is considered the gold standard for non-invasive virtual histological discrimination of different tissues.

The aim of the present study was to compare the MRI signal of the lung with chest HRCT features of SSc patients,

to analyse its correlation with other ILD clinical and instrumental parameters, and to evaluate the role of MRI in the prediction of ILD clinical progression.

Materials and methods

Patient population

This was a prospective study enrolling consecutive patients attending the Rheumatology outpatient clinic of the Azienda Ospedaliero-Universitaria Careggi, Florence, with the following inclusion criteria: (1) a diagnosis of SSc according to the 2013 ACR/EULAR classification criteria [14]; (2) a clinical indication to cardiac MRI evaluation; (3) a clinical indication to chest HRCT [5]; (4) MRI and HRCT done on the same day; (5) cardiac MRI axial acquisition on the same lung zones of HRCT. Data regarding demographic, clinical, serological, and instrumental features of the disease were collected from medical history charts, in particular regarding as follows: previous/ongoing tobacco smoke exposure, skin involvement according to modified Rodnan skin score (mRSS) [15], forced vital capacity (%FVC), lung diffusion of carbon oxide (%DLco), total lung capacity (%TLC), microvascular involvement [16], presence/history of digital ulcers [17], and the number of anterior and posterior B-lines on lung ultrasound [18]. Patients were clinically followed up from the date of MRI and HRCT: according to the evolution of their lung involvement, they were divided into stable or worsened. A group of 15 healthy individuals without SSc, undergoing clinically driven cardiac MRI which in the end excluded any cardiac condition, was considered the control group. The study was approved by the local Ethical Committee Area Vasta Nord-Ovest Toscana.

High-resolution computed tomography

HRCT were performed using a spiral CT/I high-speed GEMs (General Electric Medical Systems) machine carrying multi-detector CT scanner with a 1.0–1.5-mm thick section taken at 1.0–1.25-mm intervals throughout the entire lung during inspiration in the prone position and with spiral technique in the supine position. HRCT images were semi-quantitatively scored by two thoracic radiologists, blinded to MRI as well as to other examinations and clinical findings, with specific expertise in pulmonary disease and belonging to an established multidisciplinary group consisting of pulmonology, radiology, pathology, rheumatology, and cardiology specialists (GIIP, Gruppo Interdisciplinare Interstizipatie Polmonari) [19]. The presence of ILD was

then visually scored according to the previously described semi-quantitative Scleroderma Lung Study (SLS) I score [9]. The SLS I score was performed in three zones (upper zone: extending from the apex to aortic arch; middle zone: from the aortic arch to inferior pulmonary vein; lower zone: from the inferior pulmonary veins to diaphragms) of each lung, as previously described (5). The SLS I score is a semi-quantitative scoring method where the extent of the pulmonary abnormality in each of six zones was graded using a scale from 0 to 4, as follows (0 = absent, 1 = 1–25%, 2 = 26–50%, 3 = 51–75%, and 4 = > 75%) to evaluate the four categories of parenchymal abnormalities: (1) pure GGO; (2) lung fibrosis including thickened RET, bronchiectasis, and bronchiolectasis (BB); (3) HC, (4) emphysema (EMP). The two readers scrolled all slices from the apex to the base of each HRCT scan and attributed to each of the 6 thoracic zones, the eventual presence of GGO, RET, BB, HC, or EMP, and a number from 0 to 4 according to the extent of the parenchymal abnormality.

Lung magnetic resonance imaging

MRI was performed on a 1.5-T system (SIGNA Excite HDxT, General Electronic Medical, Waukesha, WI, USA) with cardiac phased-array coil (8 channels). The lung was assessed at the end of a clinically driven cardiac MRI by axial acquisition on the same lung zones of HRCT in the supine position, with ECG gating, during inspiration. Images were acquired by:

- Triple IR; TR (related to heart rate) about 2000 ms; TE 82 ms; FoV 38 cm; TI 180 ms; ThK 8 mm with gap variable depending on the size of the lung zone (15–20 cm); 224 × 224; Nex 1; asset 2; acquisition time about 8 s for section
- T1 Map-MCine-IR (modified Cine-IR) spoiled gradient-echo sequences with TR 3 ms; TE 1.1 ms; FA° 8 ms ThK 8 mm with gap variable depending on the size of the lung zone (15–20 cm); 192 × 192, views per segment (VPS) = 32; Nex 1; asset 2; acquisition time about 8 s for section 8 s RR = 6 time required full recovery of the longitudinal magnetization
- MCine-IR sequences are repeated and at 5, 10, and 15 min post gadolinium-chelate contrast agent (CA)
- T1 Map with MCine-IR sequences (modified Cine-IR) spoiled gradient echo with TR 3 ms; TE 1.1 ms; FA° 8 ms ThK 8 with gap variable depending on the size of the lung zone (15–20 cm); 192 × 192, views per segment (VPS) = 32; Nex 1; asset 2; acquisition time about 8 s RR = 2 time required full recovery of the longitudinal magnetization

MRI images were analysed using the HIPPO SW software, developed in IDL 8.2.3, and validated by the Cardiovascular Magnetic Resonance Unit of the Fondazione Toscana G.

Monasterio. With this software, it is possible to manually draw one or more region of interest (ROI) on a DICOM image at a particular inversion time (IT), allowing the detection of the single point within the ROI signal intensity and thus calculating an intensity signal/IT curve. The same protocol was applied to SSc patients and to the control group.

Comparison between HRCT and lung MRI

All patients underwent chest HRCT and lung MRI on the same day. On MRI, ROIs were positioned to cover all 6 thoracic zones from the apex to the diaphragm, whenever possible, according to the same scheme used for the HRCT (upper zone extending from the apex to aortic arch; middle zone extending from the aortic arch to inferior pulmonary vein; lower zone extending from the inferior pulmonary veins to diaphragms). ROIs were positioned on areas of parenchymal hyperintensity whenever present at visual estimation; otherwise, they were positioned on parenchymal areas of apparent normal intensity. ROI positioning and selection were done by the same operator on all exams, blinded to HRCT and all other patients' data, apart from the initial diagnosis of SSc. ROIs' signal intensities were then measured in STIR and T1 mapping pre- and post-gadolinium sequences at 5, 10, and 15 min after CA administration.

According to the combination of HRCT/MRI features, patients were clustered as follows:

Group 1: patients with both normal HRCT and MRI, identified as patients without SSc-related ILD signs on HRCT and no visual hyperintensity on MRI (*normal*, no ILD)

Group 2: patients without SSc-related ILD signs on HRCT but areas of visual hyperintensity on MRI (*discordant*, HRCT–/MRI+)

Group 3: patients with SSc-related ILD signs on HRCT and areas of visual hyperintensity on MRI, identified as patients with SSc-related ILD (*abnormal*, ILD)

Lung ultrasound

LUS was performed on the same the day of HRCT and MRI, as previously described (11) on the antero-lateral and posterior thorax, for a total of 58 scanning sites (28 anterior scanning sites +30 posterior scanning sites), using 2.5–3.5-MHz cardiac sector transducers (2.5 cm long) on commercially available ultrasonographic equipment (Vivid i, GE/Vingmed, Milwaukee, WI, USA). Convex (3.5–6.0 MHz) or linear transducers (7.0–10.0 MHz) were used when needed to better identify pleural alterations.

B-lines were defined as discrete laser-like vertical hyperechogenic reverberation artefacts that arise from the

pleural line, extend to the bottom of the screen, and move synchronously with respiration and lung sliding [20]. In each scanning site, B-lines were quantified from 0 to 10 as previously described [21], and summed up to obtain a total number of B-lines [21, 22]. All LUS exams were done by a single operator with more than 10 years' experience in LUS, blinded to HRCT and MRI data, and to all other clinical and instrumental information apart those clearly evident from inspection.

Follow-up

Patients were followed up at regular outpatient clinic appointments every 6–12 months by an attending rheumatologist [23]. Since there is no universally accepted definition of worsening SSc-related ILD, events were classified based on an integrated evaluation of the clinical picture combined with all available predictors of progression (i.e., $\geq 10\%$ decrease in FVC, $\geq 15\%$ decrease in DLCO, extent and characteristics of disease on HRCT scan) [18]. Two physicians, blind to lung MRI data, evaluated each case separately. Patients were censored at the time of the event or at the time of the last available visits).

Table 1 Clinical characteristics of the study population

Variable	Value
Female gender (<i>n</i> , %)	28 (93.3)
Age, years (median, IQR)	47 (37–54)
Disease duration, years (median, IQR)	3 (2–5)
Diffuse skin involvement (<i>n</i> , %)	3 (10)
Modified Rodnan skin score (median, IQR)	0 (0–6.25)
Previous or ongoing smoking exposure (<i>n</i> , %)	11 (36.6)
Anti-nuclear antibodies positivity (<i>n</i> , %)	29 (96.7)
Anti-centromere antibodies positivity (<i>n</i> , %)	10 (33.3)
Anti-topoisomerase I antibodies positivity (<i>n</i> , %)	13 (43.3)
NVC Scleroderma pattern (<i>n</i> , %)	23 (76.7)
NYHA Functional class \geq III (<i>n</i> , %)	13 (43.3)
History or presence of digital ulcers (<i>n</i> , %)	7 (23.3)
Indication for CMR	
- Impairment of LV function	5 (16.7)
- Significant arrhythmias	9 (30.0)
- Suspicion of myocarditis	3 (10.0)
- Unexplained symptoms	13 (43.3)
Presence of LGE in T1 sequence (<i>n</i> , %)	10 (33.3)
Presence of MO in T2 sequence (<i>n</i> , %)	1 (3.3)

CMR, cardiac magnetic resonance; LGE, late gadolinium enhancement; IQR, inter-quartile range; MO, myocardial oedema; NVC, nail-fold videocapillaroscopy; NYHA, New York Heart Association

Statistical analysis

Continuous variables were expressed as mean \pm standard deviation or as median and inter-quartile range (IQR), as appropriate according to normal distribution. Two-sample comparisons were performed using *t* test if variables were normally distributed and the Mann-Whitney *U* test for non-normally distributed data. Differences between baseline and each experimental point were tested using one-way analysis of variance followed by Tukey's post hoc test. Correlations between STIR and T1 signals and abovementioned clinical-instrumental parameters were tested with Pearson's or Spearman's rho test, as appropriate. Differences between groups were analysed with the ANOVA univariate test or Kruskal-Wallis test for independent samples, as applicable. The association of selected variables with the outcome was assessed by Cox's proportional hazard model using univariable and multivariable procedures. The best threshold for STIR values to predict pulmonary worsening was determined using receiver operating characteristic (ROC) curve by the Youden index; the results are expressed in terms of area under the curve (AUC) and the 95% confidence interval for this area. The event rates were estimated with Kaplan-Meier curves and compared by the log-rank test. A *p* value of <0.05 was considered statistically significant. All statistical analyses were performed using the Statistical Package for the Social Sciences (SPSS Inc., version 22, Chicago, IL, version 20) and GraphPad Prism version 6 (GraphPad Software Inc., San Diego, CA, USA).

Results

Thirty SSc patients (28 women, median age 47 (IQR 37–54) years, median disease duration 3 (IQR 2–5) years) were enrolled: 11 had previous or ongoing smoking exposure, 13 showed a NYHA class ≥ 2 , 3 presented diffuse cutaneous skin involvement, and 7 had a current or previous history of digital ulcers. Anti-nuclear, anti-centromere, and anti-topoisomerase I autoantibodies were positive in 29, 10, and 13 patients, respectively. Microvascular involvement on nail-fold videocapillaroscopy was characterized as 7 no specific, 11 early, 9 active, and 3 late patterns. More epidemiological, clinical, and instrumental details are presented in Table 1.

Comparison between HRCT and lung MRI

HRCT showed absence of ILD in 17 patients and signs of ILD in 13 patients. The SLS I score ranged from 0 to 16. From a visual point-of-view, the lung parenchyma qualitatively appeared with normal intensity on MRI in 10 cases (all corresponding to patients with absence of ILD at HRCT), whereas in 20 cases, MRI showed some degree of hyperintensity of the

Table 2 Pulmonary functional, ultrasonographic, and MRI features of the patients' groups

	All study population (30 pts)	Group 1 (10 pts)	Group 2 (7 pts)	Group 3 (13 pts)	<i>p</i> value between the three groups
Forced vital capacity, % (mean ± SD)	106 ± 21	117 ± 19	101 ± 14	97 ± 23	0.137
DLco, % (mean ± SD)	77 ± 14	87 ± 9	80 ± 13	69 ± 14	0.006
Total lung capacity, % (mean ± SD)	98 ± 15	106 ± 11	98 ± 19	91 ± 13	0.066
SLS I ILD score (median, IQR)	0 (0–5)	0 (0–0)	0 (0–0)	6 (3–12)	< 0.0001
Lung ultrasound B-lines, <i>n</i> (median, IQR)	25 (7–69)	7 (2–25)	13 (1–57)	66 (36–86)	0.002
Mean STIR values, ms (mean ± SD)	86 ± 48	35 ± 7	78 ± 23	125 ± 39	< 0.0001
T1 mapping at T0, ms (mean ± SD)	443 ± 377	0 ± 0	568 ± 404	717 ± 90	< 0.0001
T1 mapping at T5, ms (mean ± SD)	122 ± 96	0 ± 0	212 ± 65	163 ± 326	< 0.0001
T1 mapping at T10, ms (mean ± SD)	141 ± 111	0 ± 0	229 ± 76	193 ± 44	< 0.0001
T1 mapping at T15, ms (mean ± SD)	152 ± 124	0 ± 0	250 ± 87	227 ± 56	< 0.0001

DLco, lung diffusion of carbon oxide; ILD, interstitial lung disease; MRI, magnetic resonance imaging; PTS, patients; SLS, Scleroderma Lung Study

lung parenchyma. Among these patients, 13 had also evidence of ILD at HRCT, but 7 patients had a normal HRCT.

According to the previously presented combination of HRCT/MRI features, 10 patients were labelled as *normal* (group 1, both HRCT and MRI without ILD), 7 patients as *discordant* (group 2, negative HRCT but positive MRI), and 13 as *abnormal* (group 3, both positive HRCT and MRI, ILD present). Patients in the three groups were statistically different in terms of functional impairment (%FVC, %DLco, with trend towards statistical significance of %TLC), and ILD severity according to both SLS score on HRCT and number of B-lines on lung ultrasound (Table 2).

On MRI, a total of 135 ROIs were selected (mean of 4.5 ROIs per patient). Mean STIR values were significantly different among the 3 groups (Table 2, Fig. 1, and Supplementary Fig. 1). All T1 mapping pre- and post-CA values (at 5, 10, and 15 min) were also significantly different between the three groups (Table 2). In group 3, no significant differences in STIR or T1 values were found between the different ILD features (GGO, RET, and HC as seen on HRCT).

Mean STIR values showed significant correlations with SLS I score ($R = 0.79$, $p < 0.0001$), total lung ultrasound B-lines ($R = 0.73$, $p < 0.0001$) (Supplementary Fig. 2), mRSS ($R = 0.52$, $p = 0.003$), %FVC ($R = -0.46$, $p = 0.022$), and %DLco ($R = -0.63$, $p = 0.0001$). Similarly, mean T1 mapping signal at T0 (pre-CA) showed a significant correlation with SLS I score ($R = 0.52$, $p = 0.003$), lung ultrasound B-lines ($R = 0.59$, $p = 0.001$), %TLC ($R = -0.65$, $p = 0.0001$), and %DLco ($R = -0.45$, $p = 0.014$). All the ROI of the subjects of the control group yielded a STIR value of 0.

Follow-up

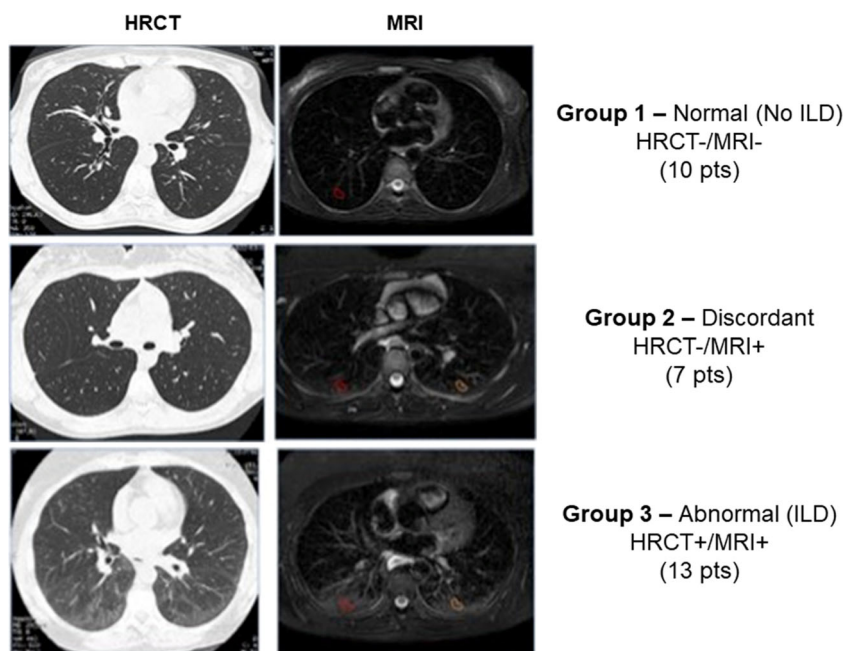
Patients were followed up for a mean of 25 ± 20 months. During this time gap, 9 patients presented worsening of lung

involvement (0/10 patient from group 1, 2/7 patients from group 2, and 7/13 patients from group 3). We found a significant difference in mean STIR values between patients with stable and worsening lung involvement, but not in T1 mapping values (both pre- and post-CA) (Table 3). At univariate analysis, mean STIR values, positivity of anti-topoisomerase I, and posterior ultrasound B-lines were significantly associated with events, with mean STIR values being the only independent predictors of events at multivariate analysis (HR 1.018; CI 1.005–1.031; $p < 0.005$ —see Table 4). ROC analysis showed an AUC for STIR values of 0.85 (0.71–0.99; $p = 0.002$). A cut-off of STIR >90 ms was then determined to maximize the sum of sensitivity and specificity, with a sensitivity and specificity of 80%. A STIR value >90 ms was thus able to discriminate patients at a higher risk of worsening pulmonary involvement (HR 8.80; CI 1.81–42.74; $p < 0.007$), as confirmed by Kaplan-Meier curves (Fig. 2).

Discussion

Our data show that lung MRI STIR and T1 values are significantly different between patients with and without SSc-related ILD. STIR values, independently of HRCT appearance, are also able to predict worsening lung involvement over time. HRCT is the gold standard to assess and quantify morphological abnormalities in SSc-related ILD, in terms of both parenchymal and vascular changes [24]. However, in the last decade, other imaging modalities have been explored to assess lung involvement, such as lung ultrasound and lung MRI, which could yield the advantage to reduce radiation exposure [25]. In previous studies, 3-T lung MRI T1-weighted sequences have been analysed in IPF: pathological areas presented a different signal intensity both pre- and post-CA administration, both when compared to non-altered areas of IPF

Fig. 1 HRCT and MRI imaging in 3 different patients of groups 1, 2, and 3



patients and to normal lung areas [26]. Previously, MRI has been tested in SSc-ILD showing interstitial modifications with a good inter- and intra-observer agreement for the measurement of ILD extent [27]. Our study confirms the potential role of lung MRI in the detection of ILD in SSc patients. In addition to previous results, we measured resonance signal intensity in STIR and T1-weighted sequences in anatomical sections corresponding to normal lung parenchyma and ILD. We found a significant difference, in either STIR or T1 values, between normal and pathological ILD tissue areas, with HRCT as the gold standard. This was further supported by the significant correlations with other functional (%FVC, %TLC, %DLco), imaging (lung ultrasound B-lines), and radiological (HRCT SLS I score) parameters reflecting SSc-ILD. The differences in T1 values of pathological and normal lung parenchyma could be explained by differences in proton density and tissue composition, likely related to the higher percentage of water and proteins in inflamed areas or increase of macro-molecule fraction and water decrease content in fibrotic areas [28].

Moreover, we identified a group of patients with apparently no signs of ILD on HRCT but with signal intensity abnormalities at lung MRI. This group, while not showing clear ILD features, does not seem completely normal, with intermediate values of STIR and T1 at MRI, as well as %FVC, %DLco, and lung ultrasound B-lines. This evidence could be related to a higher sensitivity but lower specificity of quantitative lung MRI and lung ultrasound when compared to visual estimation of HRCT. Another possible explanation which could account for the apparent discrepancy between HRCT and MRI results could be related to the transient accumulation of extravascular lung water in the dependent areas of the lung, due to the supine position, determining increased STIR and T1 values compared to the normally aerated lung parenchyma. In fact, Stadler et al. have shown that T1 value after CA administration was higher in posterior versus anterior lung areas, possibly related to the pooling of blood in the supine position [29]. In our patients, MRI was performed in full inspiration, with reduction of proton density within the ROIs and consequently lower signal-to-noise ratio in the normal lung. Similar findings

Table 3 Baseline MRI values according to worsening of lung involvement

	Stable lung involvement (21 pts)	Worsening lung involvement (9 pts)	<i>p</i> value
Mean STIR values, ms (mean ± SD)	66 ± 37	129 ± 51	0.003
T1 mapping at T0, ms (mean ± SD)	268 ± 410	578 ± 376	0.119
T1 mapping at T5, ms (mean ± SD)	102 ± 103	131 ± 73	0.382
T1 mapping at T10, ms (mean ± SD)	118 ± 118	156 ± 90	0.334
T1 mapping at T15, ms (mean ± SD)	133 ± 133	195 ± 117	0.241

MRI, magnetic resonance imaging

Table 4 Univariate and multivariate regression to predict for worsening lung involvement

	HR (95% CI)	<i>p</i> value	HR (95% CI)	<i>p</i> value
NYHA class	0.627 (0.165–2.379)	0.493		
Modified Rodnan skin score	1.039 (0.965–1.119)	0.311		
Anti-topoisomerase I positivity	5.223 (1.134–26.889)	0.034	2.389 (0.981–16.788)	0.381
FVC%	0.982 (0.955–1.010)	0.206		
DLco%	0.960 (0.917–1.005)	0.079		
Lung ultrasound posterior B-lines	1.031 (1.002–1.062)	0.039	1.022 (0.981–1.064)	0.298
SLS I ILD score	1.082 (0.978–1.196)	0.124		
Mean STIR values	1.016 (1.005–1.028)	0.005	1.018 (1.005–1.031)	0.005
T1 mapping at T0	1.002 (1.000–1.004)	0.096		

FVC, forced vital capacity; DLco, lung diffusion of carbon oxide; SLS, Scleroderma Lung Study; ILD, interstitial lung disease

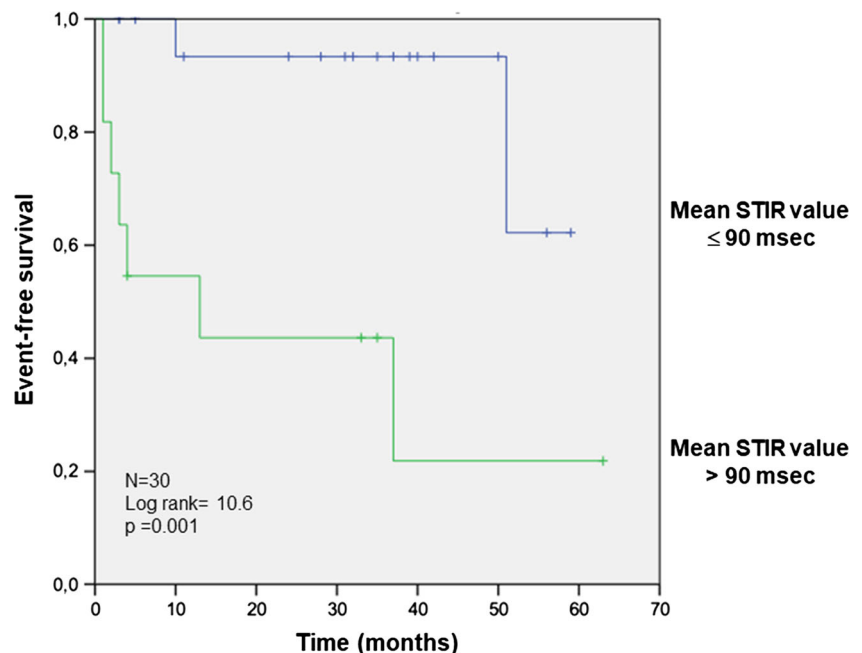
were previously reported in 24 SSc patient with T2 sequence MRI: in the 2 cases of positive MRI but negative HRCT, the authors speculated on the possible detection by MRI of a very early non-HRCT-detectable GGO; however, they considered these two cases as false positive for MRI, given the presence of false positive also in the control group, differently from our cohort, where all control subjects without SSc had no increased STIR signal on the lung parenchyma [30].

Our data show significant correlations between MRI findings and ILD signs as assessed by other tools. Mean STIR and mean T1 values correlated with %TLC and %DLco. This is in agreement with the results of Pinal-Fernandez et al. who showed a significant correlation between MRI evaluation of ILD extent and respiratory functional parameters [27]. These data confirm also those of Ohno et al. who showed that mean T2 values are different when comparing connective tissue

disease ILD and healthy subjects, with significant correlation with %DLco and severity of ILD on HRCT [31]. Moreover, the correlations found with lung ultrasound B-lines further support the role of non-radiating tools in evaluating lung involvement.

To the best of our knowledge, these are the first data showing promising results of the use of lung MRI in predicting future clinical worsening related to lung involvement. In SSc, the capacity to identify patients characterized by a progressive evolution still remains one of the main clinical unmet needs [23]. In our cohort, STIR values were the only parameter, among all the clinical and instrumental data available, which was able to predict further ILD development or worsening, irrespective of the presence of overt ILD at HRCT (group 2 with discordant normal HRCT and hyperintensity on MRI).

Fig. 2 Kaplan-Meier curves to predict lung worsening during follow-up in patients with mean STIR value ≤ and > 90 ms



Our data should be considered preliminary because the study has some limitations. The study population is not large, and MRI was performed in the supine position only, in order to examine the myocardial status. This position is not ideal to discriminate dependent areas with increased signal due to the patient's position. Moreover, some details concerning MRI methodology need to be tested and further verified on a much larger population to identify the best setting for the ILD investigation. Finally, our population presented at baseline relatively preserved lung function in terms of both FVC% and TLC%, while mean %DLco values already showed a borderline impairment. This could be representative of the early signs of ILD, without significant restrictive impairment both at baseline and during follow-up assessments, which may be more frequent in advanced and rapidly progressive cases.

In conclusion, lung MRI is a promising technique which might be able to discriminate patients with normal lung parenchyma from patients with SSc-ILD, and to identify altered signal intensities in lung parenchyma areas that appear normal on HRCT.

These preliminary data support the scientific effort to better understand the potentiality of lung MRI which, in the future, could help selecting patients for an early personalized treatment of SSc-related ILD [32, 33], as well as a more appropriate use of HRCT, in order to reduce radiation exposure [34], in particular in young fertile patients.

Supplementary Information The online version contains supplementary material available at <https://doi.org/10.1007/s10067-020-05491-9>.

Acknowledgements We thank Claudia Santarlasci and Gennaro D'Angelo for their precious technical support.

Authors' contribution Luna Gargani contributed to the conception of the study, data acquisition, analysis and interpretation, and work drafting and gave final approval of the version to be published. She is the guarantor of the paper, taking responsibility for the integrity of the work as a whole, from inception to published article.

Cosimo Bruni contributed to data acquisition, analysis and interpretation, and text drafting and gave final approval of the version to be published.

Daniele De Marchi reviewed and scored the MRI scan, contributed to data analysis and interpretation and text drafting, and gave final approval of the version to be published.

Chiara Romei reviewed and scored the HRCT scans, contributed to data analysis and interpretation and text drafting, and gave final approval of the version to be published.

Serena Guiducci contributed to data acquisition, analysis and interpretation, and text drafting and gave final approval of the version to be published.

Silvia Bellando-Randone contributed to data acquisition, analysis and interpretation, and text drafting and gave final approval of the version to be published.

Giovanni Donato Aqauro contributed to data acquisition, analysis and interpretation, and text drafting and gave final approval of the version to be published.

Alessia Pepe contributed to data acquisition, analysis and interpretation, and text drafting and gave final approval of the version to be published.

Emanuele Neri contributed to data analysis and interpretation and text drafting and gave final approval of the version to be published.

Stefano Colagrande contributed to data analysis and interpretation and text drafting and gave final approval of the version to be published.

Fabio Falaschi reviewed and scored the HRCT scans, contributed to data analysis and interpretation, and text drafting, and gave final approval of the version to be published.

Alessandro Pingitore reviewed and scored the MRI scan, contributed to data analysis and interpretation, and text drafting, and gave final approval of the version to be published.

Alberto Moggi-Pignone contributed to data analysis and interpretation and text drafting and gave final approval of the version to be published.

Marco Matucci-Cerinic contributed to the conception of the study, data interpretation, and work drafting and gave final approval of the version to be published.

Data availability Data are available upon reasonable request.

Compliance with ethical standards

Competing interests Luna Gargani declares consultancy honoraria from GE Healthcare (not related to the topic of this manuscript); no conflicts of interest for the other authors.

Ethical approval information Received from the Local Ethical Committee Area Vasta Nord-Ovest (n°2849).

Patient and public involvement Patients or the public were not involved in the design, or conduct, or reporting, or dissemination plans of our research.

References

- Nihtyanova SI, Denton CP (2020) Pathogenesis of systemic sclerosis associated interstitial lung disease. *Journal of Scleroderma and Related Disorders* 5(2_suppl):6–16. <https://doi.org/10.1177/2397198320903867>
- Varga J, Trojanowska M, Kuwana M (2017) Pathogenesis of systemic sclerosis: recent insights of molecular and cellular mechanisms and therapeutic opportunities. *Journal of Scleroderma and Related Disorders* 2(3):137–152. <https://doi.org/10.5301/jsrd.5000249>
- Volkman ER, Fischer A Update on morbidity and mortality in systemic sclerosis-related interstitial lung disease. *Journal of Scleroderma and Related Disorders* 0 (0):2397198320915042. doi:<https://doi.org/10.1177/2397198320915042>
- Barsotti S, Bruni C, Orlandi M, Della Rossa A, Marasco E, Codullo V, Guiducci S (2017) One year in review 2017: systemic sclerosis. *Clin Exp Rheumatol* 35 Suppl 106(4):3–20
- Hoffmann-Vold A-M, Maher TM, Philpot EE, Ashrafzadeh A, Barake R, Barsotti S, Bruni C, Carducci P, Carreira PE, Castellví I, Del Galdo F, Distler JHW, Foeldvari I, Fraticelli P, George PM, Griffiths B, Guillén-Del-Castillo A, Hamid AM, Horváth R, Hughes M, Kreuter M, Moazedi-Fuerst F, Olas J, Paul S, Rotondo C, Rubio-Rivas M, Seferian A, Tomčík M, Uzunhan Y, Walker UA, Więsik-Szewczyk E, Distler O (2020) The identification and management of interstitial lung disease in systemic sclerosis: evidence-based European consensus statements. *The Lancet*

- Rheumatology 2(2):e71–e83. [https://doi.org/10.1016/S2665-9913\(19\)30144-4](https://doi.org/10.1016/S2665-9913(19)30144-4)
6. Volkmann ER, Chung A, Tashkin DP (2017) Managing systemic sclerosis-related interstitial lung disease in the modern treatment era. *Journal of Scleroderma and Related Disorders* 2(2):72–83. <https://doi.org/10.5301/jrsd.5000237>
 7. Smith V, Scire CA, Talarico R, Airo P, Alexander T, Allamore Y, Bruni C, Codullo V, Dalm V, De Vries-Bouwstra J, Della Rossa A, Distler O, Galetti I, Launay D, Lepri G, Mathian A, Mouthon L, Ruaro B, Sulli A, Tincani A, Vandecasteele E, Vanhaecke A, Vanthuyne M, Van den Hoogen F, Van Vollenhoven R, Voskuyl AE, Zanatta E, Bombardieri S, Burmester G, Eurico FJ, Frank C, Hachulla E, Houssiau F, Mueller-Ladner U, Schneider M, van Laar JM, Vieira A, Cutolo M, Mosca M, Matucci-Cerinic M (2018) Systemic sclerosis: state of the art on clinical practice guidelines. *RMD Open* 4(Suppl 1):e000782. <https://doi.org/10.1136/rmdopen-2018-000782>
 8. Hartman TE, Swensen SJ, Hansell DM, Colby TV, Myers JL, Tazelaar HD, Nicholson AG, Wells AU, Ryu JH, Midthun DE, du Bois RM, Muller NL (2000) Nonspecific interstitial pneumonia: variable appearance at high-resolution chest CT. *Radiology* 217(3):701–705. <https://doi.org/10.1148/radiology.217.3.r00nv31701>
 9. Goldin JG, Lynch DA, Strollo DC, Suh RD, Schraufnagel DE, Clements PJ, Elashoff RM, Furst DE, Vasunilashorn S, MF MN-G, Brown MS, Roth MD, Tashkin DP, Scleroderma Lung Study Research G (2008) High-resolution CT scan findings in patients with symptomatic scleroderma-related interstitial lung disease. *Chest* 134(2):358–367. <https://doi.org/10.1378/chest.07-2444>
 10. Biederer J, Mirsadraee S, Beer M, Molinari F, Hintze C, Bauman G, Both M, Van Beek EJ, Wild J, Puderbach M (2012) MRI of the lung (3/3)-current applications and future perspectives. *Insights Imaging* 3(4):373–386. <https://doi.org/10.1007/s13244-011-0142-z>
 11. Romei C, Turturici L, Tavanti L, Miedema J, Fiorini S, Marletta M, Wielopolski P, Tiddens H, Falaschi F, Ciet P (2018) The use of chest magnetic resonance imaging in interstitial lung disease: a systematic review. *Eur Respir Rev* 27(150). <https://doi.org/10.1183/16000617.0062-2018>
 12. Lonzeiti L, Zanon M, Pacini GS, Altmayer S, Martins de Oliveira D, Rubin AS, Gazzoni FF, Barros MC, Hochhegger B (2019) Magnetic resonance imaging of interstitial lung diseases: a state-of-the-art review. *Respir Med* 155:79–85. <https://doi.org/10.1016/j.rmed.2019.07.006>
 13. Wild JM, Marshall H, Bock M, Schad LR, Jakob PM, Puderbach M, Molinari F, Van Beek EJ, Biederer J (2012) MRI of the lung (1/3): methods. *Insights Imaging* 3(4):345–353. <https://doi.org/10.1007/s13244-012-0176-x>
 14. van den Hoogen F, Khanna D, Fransen J, Johnson SR, Baron M, Tyndall A, Matucci-Cerinic M, Naden RP, Medsger TA Jr, Carreira PE, Riemekasten G, Clements PJ, Denton CP, Distler O, Allamore Y, Furst DE, Gabrielli A, Mayes MD, van Laar JM, Seibold JR, Czirjak L, Steen VD, Inanc M, Kowal-Bielecka O, Muller-Ladner U, Valentini G, Veale DJ, Vonk MC, Walker UA, Chung L, Collier DH, Csuka ME, Fessler BJ, Guiducci S, Herrick A, Hsu VM, Jimenez S, Kahaleh B, Merkel PA, Sierakowski S, Silver RM, Simms RW, Varga J, Pope JE (2013) 2013 classification criteria for systemic sclerosis: an American College of Rheumatology/European league against rheumatism collaborative initiative. *Arthritis Rheum* 65(11):2737–2747. <https://doi.org/10.1002/art.38098>
 15. Showalter K, Merkel PA, Khanna D, Gordon JK (2020) Assessment of skin disease in scleroderma: practices and opinions of investigators studying scleroderma. *Journal of Scleroderma and Related Disorders* 5(3):167–171. <https://doi.org/10.1177/2397198320921044>
 16. Ruaro B, Nallino MG, Casabella A, Salton F, Confalonieri P, De Tanti A, Bruni C (2020) Monitoring the microcirculation in the diagnosis and follow-up of systemic sclerosis patients: focus on pulmonary and peripheral vascular manifestations. *Microcirculation*. doi:<https://doi.org/10.1111/micc.12647>
 17. Suliman YA, Bruni C, Johnson SR, Praino E, Alemam M, Borazan N, Cometi L, Myers B, Khanna D, Allamore Y, Baron M, Krieg T, Herrick A, Afonso A, Distler O, Kafaja S, Denton CP, Matucci-Cerinic M, Furst DE (2017) Defining skin ulcers in systemic sclerosis: systematic literature review and proposed world Scleroderma Foundation (WSF) definition. *Journal of Scleroderma and Related Disorders* 2(2):115–120. <https://doi.org/10.5301/jrsd.5000236>
 18. Barskova T, Gargani L, Guiducci S, Randone SB, Bruni C, Carnesecchi G, Conforti ML, Porta F, Pignone A, Caramella D, Picano E, Cerinic MM (2013) Lung ultrasound for the screening of interstitial lung disease in very early systemic sclerosis. *Ann Rheum Dis* 72(3):390–395. <https://doi.org/10.1136/annrheumdis-2011-201072>
 19. Hoffmann-Vold AM, Allamore Y, Bendstrup E, Bruni C, Distler O, Maher TM, Wijssenbeek M, Kreuter M (2020) The need for a holistic approach for SSc-ILD - achievements and ambiguity in a devastating disease. *Respir Res* 21(1):197. <https://doi.org/10.1186/s12931-020-01459-0>
 20. Picicelli G, Elbarbary M, Blaivas M, Lichtenstein DA, Mathis G, Kirkpatrick AW, Melniker L, Gargani L, Noble VE, Via G, Dean A, Tsung JW, Soldati G, Copetti R, Bouhemad B, Reissig A, Agricola E, Rouby JJ, Arbelot C, Liteplo A, Sargsyan A, Silva F, Hoppmann R, Breitkreutz R, Seibel A, Neri L, Storti E, Petrovic T, International Liaison Committee on Lung Ultrasound for International Consensus Conference on Lung U (2012) International evidence-based recommendations for point-of-care lung ultrasound. *Intensive Care Med* 38(4):577–591. <https://doi.org/10.1007/s00134-012-2513-4>
 21. Gargani L, Bruni C, Romei C, Frumento P, Moreo A, Agoston G, Guiducci S, Bellando-Randone S, Lepri G, Belloli L, Della Rossa A, Delle Sedie A, Stagnaro C, De Nes M, Salvadori S, Mosca M, Falaschi F, Epis O, Picano E, Matucci-Cerinic M (2020) Prognostic value of lung ultrasound B-lines in systemic sclerosis. *Chest*. <https://doi.org/10.1016/j.chest.2020.03.075>
 22. Gargani L (2019) Ultrasound of the lungs: more than a room with a view. *Heart Fail Clin* 15(2):297–303. <https://doi.org/10.1016/j.hfc.2018.12.010>
 23. Volkmann ER (2020) Natural history of systemic sclerosis-related interstitial lung disease: how to identify a progressive fibrosing phenotype. *Journal of Scleroderma and Related Disorders* 5(2_suppl):31–40. <https://doi.org/10.1177/2397198319889549>
 24. Occhipinti M, Bruni C, Camiciottoli G, Bartolucci M, Bellando-Randone S, Bassetto A, Cuomo G, Giuggioli D, Ciardi G, Fabbri A, Tomassetti S, Lavorini F, Pistolesi M, Colagrande S, Matucci-Cerinic M (2020) Quantitative analysis of pulmonary vasculature in systemic sclerosis at spirometry-gated chest CT. *Ann Rheum Dis*. <https://doi.org/10.1136/annrheumdis-2020-217359>
 25. Picano E, Semelka R, Ravenel J, Matucci-Cerinic M (2014) Rheumatological diseases and cancer: the hidden variable of radiation exposure. *Ann Rheum Dis* 73(12):2065–2068. <https://doi.org/10.1136/annrheumdis-2014-206585>
 26. Mirsadraee S, Tse M, Kershaw L, Semple S, Schembri N, Chin C, Murchison JT, Hirani N, van Beek EJ (2016) T1 characteristics of interstitial pulmonary fibrosis on 3T MRI—a predictor of early interstitial change?. *Quant Imaging Med Surg* 6(1):42–49. doi:<https://doi.org/10.3978/j.issn.2223-4292.2016.02.02>
 27. Pinal-Fernandez I, Pineda-Sanchez V, Pallisa-Nunez E, Simeon-Aznar CP, Selva-O'Callaghan A, Fonollosa-Pla V, Vilardell-Tarres M (2016) Fast 1.5 T chest MRI for the assessment of interstitial lung disease extent secondary to systemic sclerosis. *Clin Rheumatol* 35(9):2339–2345. <https://doi.org/10.1007/s10067-016-3267-0>

28. Ganesan KAD, Hackmann A, Laicher G, Chan P, Cutillo AG (1996) NMR relaxation and water self-diffusion mechanisms in lung. In: Cutillo AG e (ed) applications of magnetic resonance to the study of the lung. Futura, New York, pp 115–139
29. Stadler A, Jakob PM, Griswold M, Barth M, Bankier AA (2005) T1 mapping of the entire lung parenchyma: influence of the respiratory phase in healthy individuals. *J Magn Reson Imaging* 21(6):759–764. <https://doi.org/10.1002/jmri.20319>
30. Muller CS, Warszawiak D, Paiva EDS, Escuissato DL (2017) Pulmonary magnetic resonance imaging is similar to chest tomography in detecting inflammation in patients with systemic sclerosis. *Rev Bras Reumatol Engl Ed* 57(5):419–424. <https://doi.org/10.1016/j.rbre.2017.02.001>
31. Ohno Y, Nishio M, Koyama H, Takenaka D, Takahashi M, Yoshikawa T, Matsumoto S, Obara M, van Cauteren M, Sugimura K (2013) Pulmonary MR imaging with ultra-short TEs: utility for disease severity assessment of connective tissue disease patients. *Eur J Radiol* 82(8):1359–1365. <https://doi.org/10.1016/j.ejrad.2013.02.031>
32. Roofeh D, Distler O, Allanore Y, Denton CP, Khanna D (2020) Treatment of systemic sclerosis-associated interstitial lung disease: lessons from clinical trials. *Journal of Scleroderma and Related Disorders* 5(2_suppl):61–71. <https://doi.org/10.1177/2397198320903208>
33. Lepri G, Hughes M, Bruni C, Cerinic MM, Randone SB (2020) Recent advances steer the future of systemic sclerosis toward precision medicine. *Clin Rheumatol* 39(1):1–4. <https://doi.org/10.1007/s10067-019-04834-5>
34. Picano E, Matucci-Cerinic M (2011) Unnecessary radiation exposure from medical imaging in the rheumatology patient. *Rheumatology (Oxford)* 50(9):1537–1539. <https://doi.org/10.1093/rheumatology/keq412>

Publisher's note Springer Nature remains neutral with regard to jurisdictional claims in published maps and institutional affiliations.